Electronic Supplementary Material (ESI) for ChemComm.
This journal is © The Royal Society of Chemistry 2019

Electronic Supporting Information for:

High Affinity Threading of New Tetralactam Macrocycle in Water by Fluorescent Deep-Red and Near-Infrared Squaraine Dyes

Janel M. Dempsey,[1] Canjia Zhai,[1] Hannah H. McGarraugh,[1] Cynthia L. Schreiber, [1] Shannon E. Stoffel,[1] Andrew Johnson,[2] Bradley D. Smith[1]*

1. Department of Chemistry and Biochemistry, 236 Nieuwland Science Hall, University of Notre Dame, Notre Dame, IN 46556, USA

2. Division of Science, 317 Fugitte Science Center, Lindsey Wilson College, Columbia, KY 42728, USA

*Email: smith.115@nd.edu

Contents:

A. Materials……S2
B. Synthesis……..……..S3
C. ^{1}H and ^{13}C NMR Spectra……..……...……...S5
D. Evidence for Squaraine and Croconaine Threading of M3…….……S8
E. Competitive Macrocycle Threading Experiments……...…..S14
F. Threading Association Constant Measurements……..…S19
G. Threading Rate Constant Measurements……...S26
H. Molecular Dynamics Simulations of Threaded Complex…...…….……S29
I. References……...…….....S30

A. Materials

All chemicals and solvents were purchased as reagent grade and used without further purification unless otherwise noted. Reactions were monitored by TLC plate (precoated with 60 Å silica gel, F254) purchased from SILICYCLE and visualized by UV light (254, 365 nm) or $KMnO_4$ stain. Flash column chromatography was performed using silica gel (silicaFlash P60 from SILICYCLE) as the stationary phase. ^{1}H and ^{13}C NMR spectra were recorded on Bruker AVANCE III HD 400 and 500 MHz spectrometers at 25 °C. Chemical shift is presented in ppm and referenced by residual solvent peak. Mass spectrometry (MS) was performed using a Bruker microTOF II spectrometer. Absorption spectra were collected using an Evolution 201 UV-Vis Spectrometer with ThermoInsight software. Fluorescence spectra were collected using a Horiba Fluoromax-4 Fluorometer with FluorEssence software. Bis(aminomethyl)durene **1**;[S1] 5-(prop-2-yn-1-yloxy)isophthaloyl dichloride **2**;[S2] azide dendrimer **4**;[S3] macrocycles **M1**[S4] and **M2**;[S1] water-soluble squaraines **MeSQ700**,[S5] **EtSQ700**,[S6] **PrSQ700**,[S5] **EtSQ800**,[S7] and **BzSQ700**;[S8] and water-soluble croconaine **MeCR800**[S9] were synthesized according to previously published procedures.

B. Synthesis

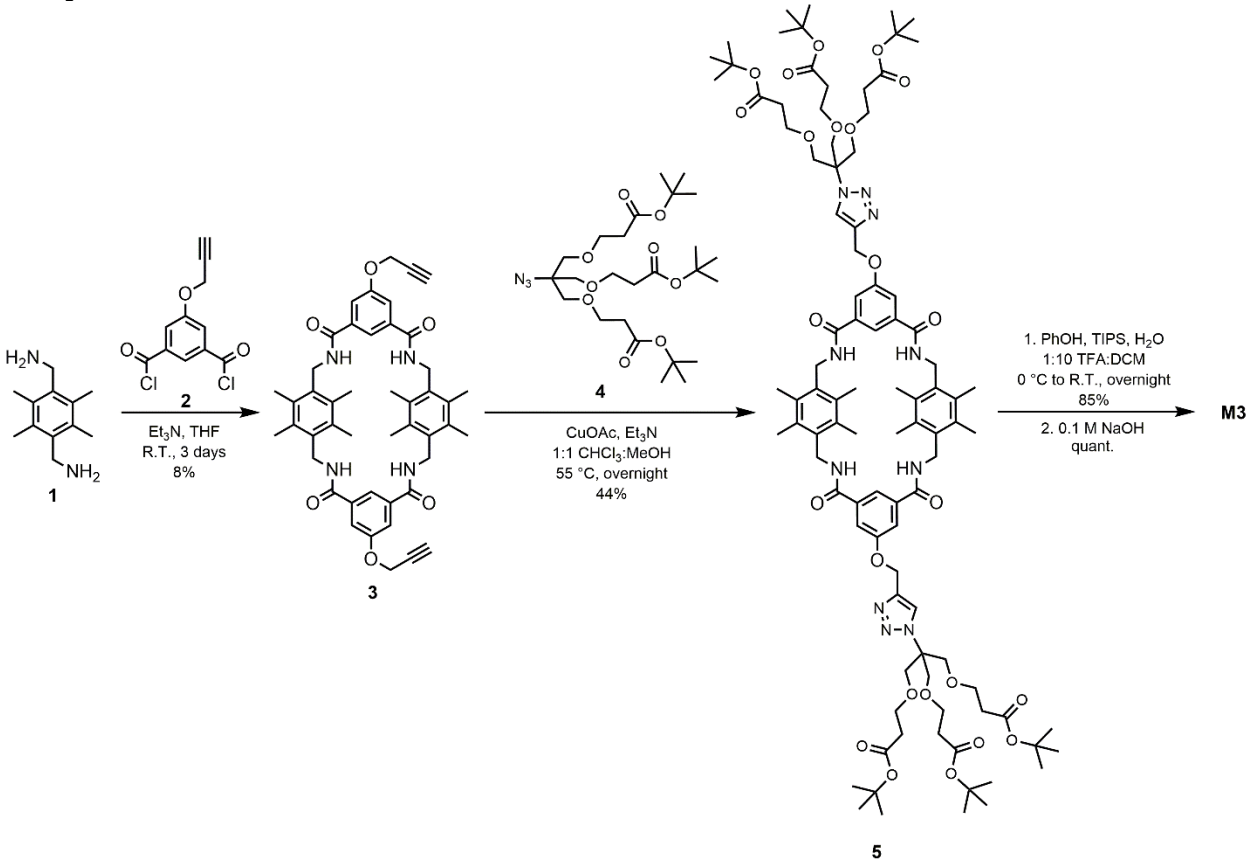

Scheme S1: Synthesis of water-soluble macrocycle **M3** by copper-catalyzed azide-alkyne cycloaddition (CuAAC) reaction.

Compound 3. A solution of acid chloride **2** (133.7 mg, 0.520 mmol) in THF (50 mL) was added dropwise by syringe pump to a solution of compound **1** (100 mg, 0.520 mmol) and triethylamine (0.6 mL) in THF (200 mL) over 12 hours. The solution was then stirred at room temperature for 3 days under nitrogen. The solvent was removed by rotary evaporation and the residue was dissolved in $CHCl_3$ and filtered. The solvent was removed from the filtrate by rotary evaporation. The residue was then purified by column chromatography (0-10% acetone in CH_2Cl_2) to obtain the crude product, which was then further washed with acetone to obtain compound **3** as a white powder (16.5 mg, 8%). ^{1}H NMR (500 MHz, $CDCl_3$, 25 °C): δ 7.87 (s, 4H), 7.13 (s, 2H), 6.01 (d, *J* = 4.7 Hz, 4H), 4.78 (d, *J* = 2.4 Hz, 4H), 4.68 (d, *J* = 4.4 Hz, 8H), 2.57 (d, *J* = 2.4 Hz, 1H), 2.27 (s, 24H). ^{13}C NMR (100 MHz, $CDCl_3$, 25 °C): δ 165.64, 135.39, 134.83, 133.50, 119.02, 77.24, 67.07, 56.21, 40.36, 32.33, 23.42, 16.61. HRMS (ESI-TOF) m/z: $[M+H]^+$ calcd for $C_{46}H_{49}N_4O_6^+$ 753.3647; found 753.3657.

Compound 5. Compound **3** (9.9 mg, 0.0131 mmol) was added into a solution of dendrimer **4** (53.2 mg, 0.100 mmol) in 1:1 $CHCl_3$:MeOH (2 mL). Triethylamine (18.2 μL, 0.131 mmol) and copper (I) acetate (18 mg, 0.147 mmol) were then added into the mixture, and the reaction was stirred at 55 °C overnight. The solvent was removed by rotary evaporation and the residue was purified by column chromatography (0-20%

acetone in CH_2Cl_2) to yield compound **5** as a colorless solid (10.6 mg, 44%). ^{1}H NMR (500 MHz, $CDCl_3$, 25 °C): δ 8.00 (s, 2H), 7.90 (s, 4H), 7.08 (s, 2H), 5.99 (s, 4H), 5.26 (s, 4H), 4.70 (d, *J* = 4.4 Hz, 8H), 3.99 (s, 12H), 3.67 (t, *J* = 6.3 Hz, 12H), 2.44 (t, *J* = 6.2 Hz, 12H), 2.31 (s, 24H), 1.44 (s, 54H). ^{13}C NMR: Small quantity of material prevented ^{13}C analysis. HRMS (ESI-TOF) m/z: $[M+H]^+$ calcd for $C_{96}H_{139}N_{10}O_{24}^+$ 1816.9990; Found 1816.9999.

Macrocycle M3. Triisopropylsilane (200 μL), H_2O (200 μL) and phenol (50 mg) were added into a solution of compound **5** (4.2 mg, 0.00231 mmol) in CH_2Cl_2 (2 mL). The mixture was then cooled to 0 °C in an ice bath. Trifluoroacetic acid (2 mL) was added dropwise into the mixture, which was then stirred at room temperature overnight. The solvent was removed by rotary evaporation and the residue was washed with diethyl ether to yield the intermediate carboxylic acid as a white solid (2.9 mg, 85%). ^{1}H NMR (500 MHz, CD_3OD, 25 °C): δ 8.22 (s, 2H), 8.02 (s, 2H), 7.80 (s, 4H), 5.31 (s, 4H), 4.56 (s, 8H), 3.99 (s, 12H), 3.68 (s, 12H), 2.48 (s, 12H), 2.19 (s, 24H). HRMS (ESI-TOF) m/z: $[M+H]^+$ calcd for $C_{72}H_{91}N_{10}O_{24}^+$ 1479.6202; Found 1479.6222. To this solid were added a few drops of H_2O, then the solution was neutralized with 0.1 M sodium hydroxide solution to pH 7. The mixture was passed through a 0.45 μm syringe filter and lyophilized to obtain macrocycle **M3** as a white solid (3.6 mg, quant.). ^{1}H NMR (500 MHz, D_2O, 25 ° C): δ 8.10 (s, 2H), 7.69 (s, 2H), 7.60 (s, 4H), 5.48 (s, 4H), 4.64 (s, 8H), 3.66 (s, 12H), 3.18 (t, *J* = 7.0 Hz, 12H), 2.15 (s, 24H), 1.93 (t, *J* = 7.0 Hz, 12H). ^{13}C NMR (125 MHz, D_2O, 25 ° C): δ 179.46, 168.17, 157.59, 142.55, 135.49, 134.73, 133.07, 124.93, 119.55, 69.81, 68.89, 68.83, 62.14, 39.16, 37.03, 15.91. (Note that one carbon signal could not be located.) HRMS (ESI-TOF) m/z: $[M-5Na+6H]^+$ calcd for $C_{72}H_{90}N_{10}NaO_{24}^+$ 1501.6022; found 1501.5992.

C. ^{1}H and ^{13}C NMR Spectra

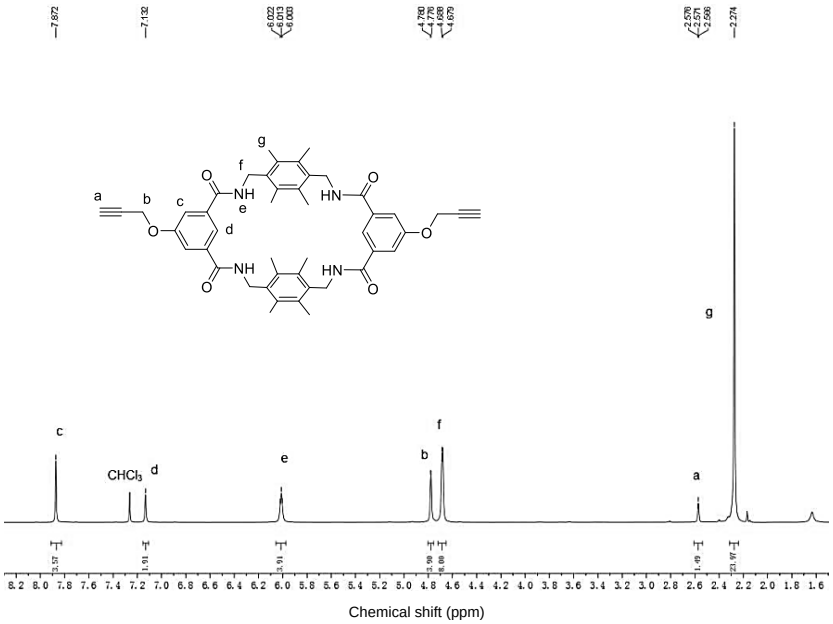

Figure S1: ^{1}H NMR (500 MHz, $CDCl_3$, 25° C) of compound **3**.

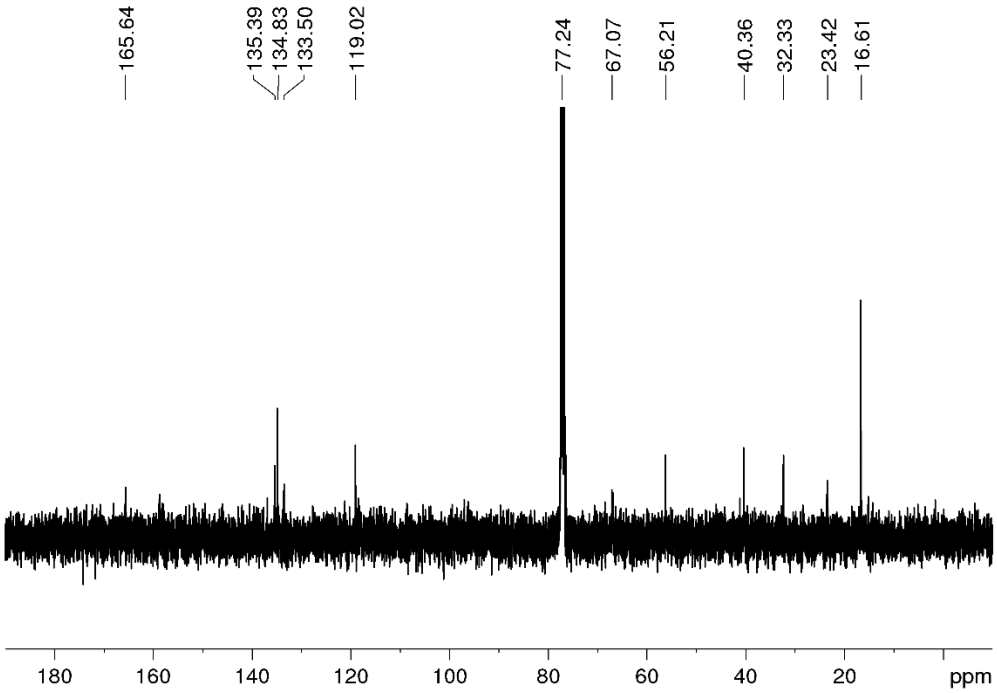

Figure S2: ^{13}C NMR (100 MHz, $CDCl_3$, 25° C) of compound **3**.

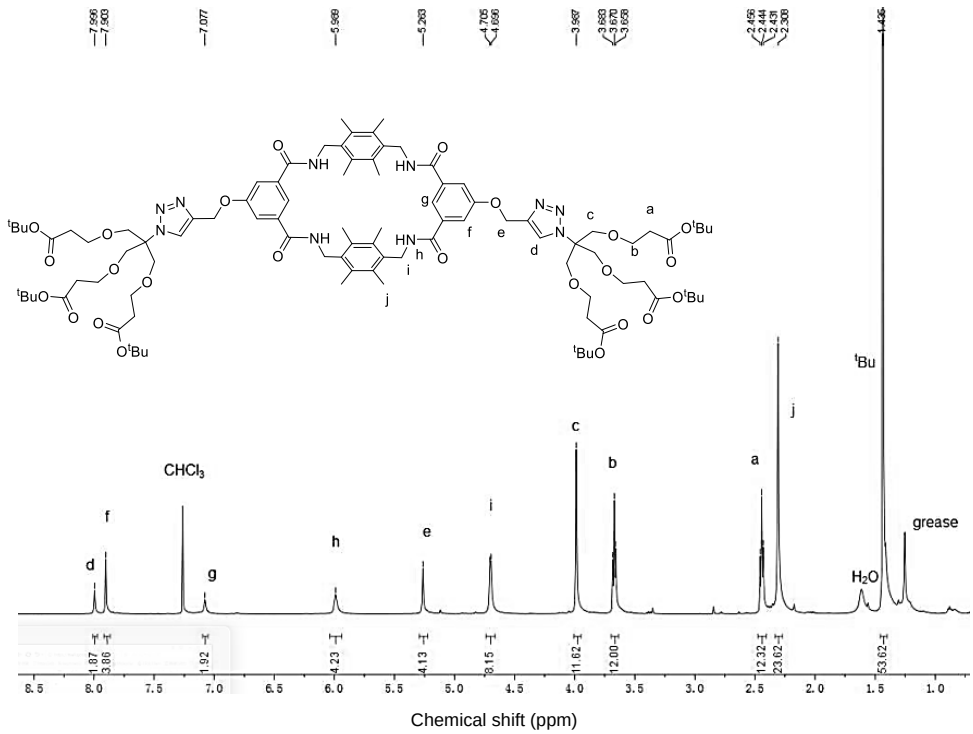

Figure S3: ^{1}H NMR (500 MHz, $CDCl_3$, 25 °C) of compound **5**.

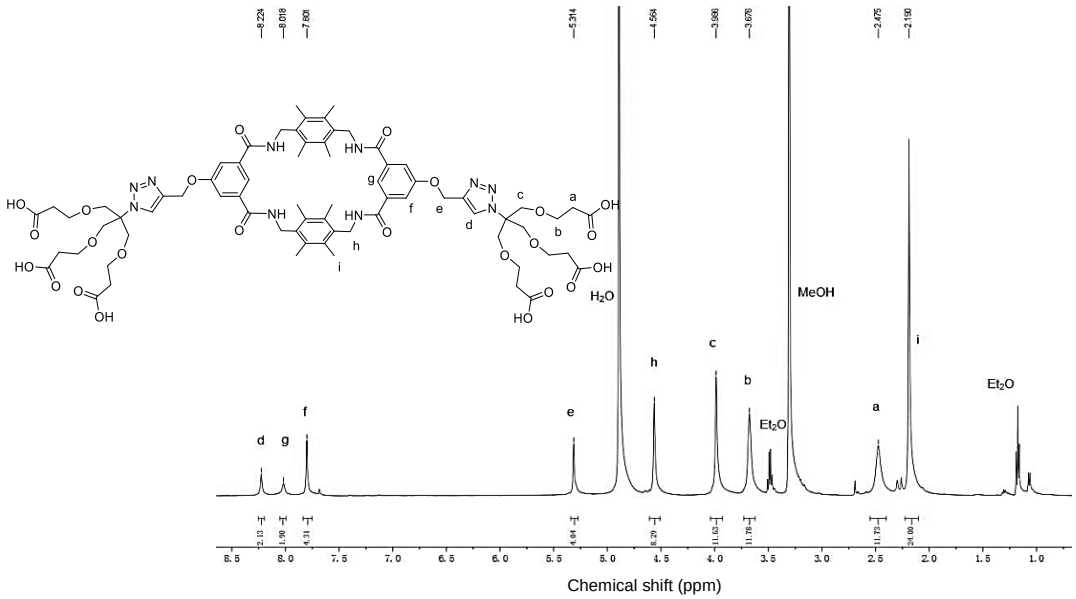

Figure S4: ^{1}H NMR (500 MHz, CD_3OD, 25 °C) of intermediate carboxylic acid.

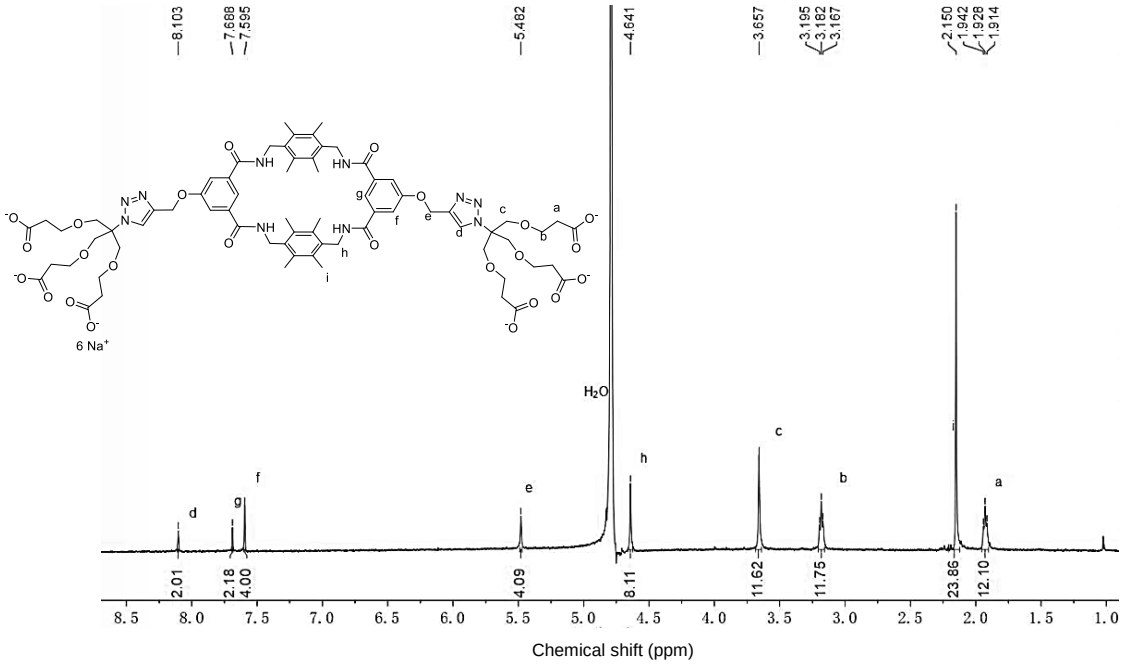

Figure S5: ^{1}H NMR (500 MHz, D_2O, 25 °C) of macrocycle **M3**.

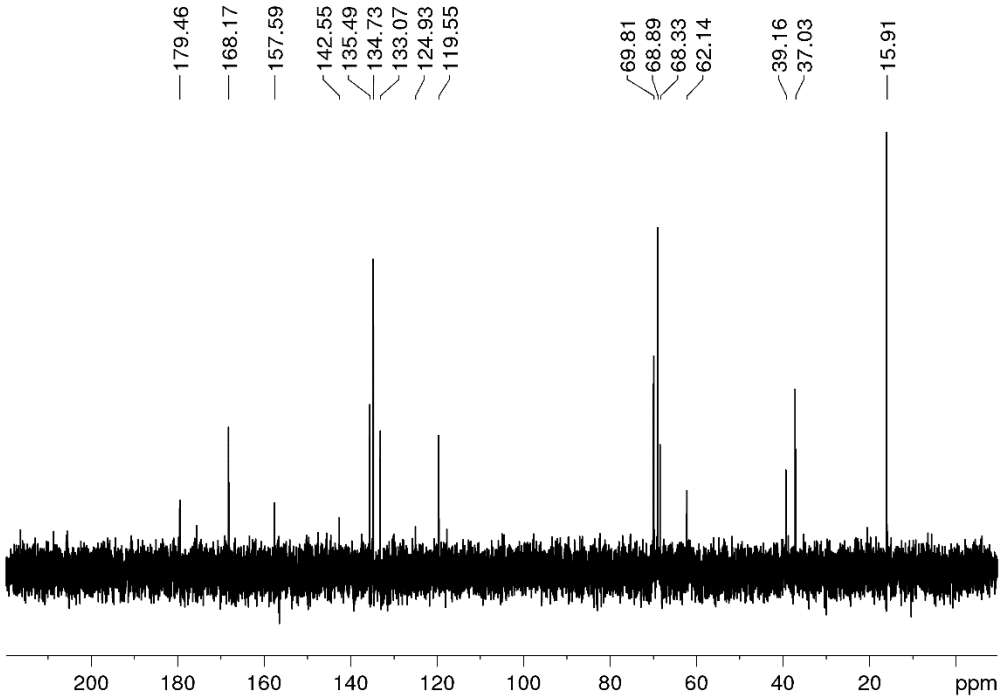

Figure S6: ^{13}C NMR (125 MHz, D_2O, 25 °C) of macrocycle **M3**.

D. Evidence for Squaraine and Croconaine Threading of M3

Changes in Absorption and Fluorescence

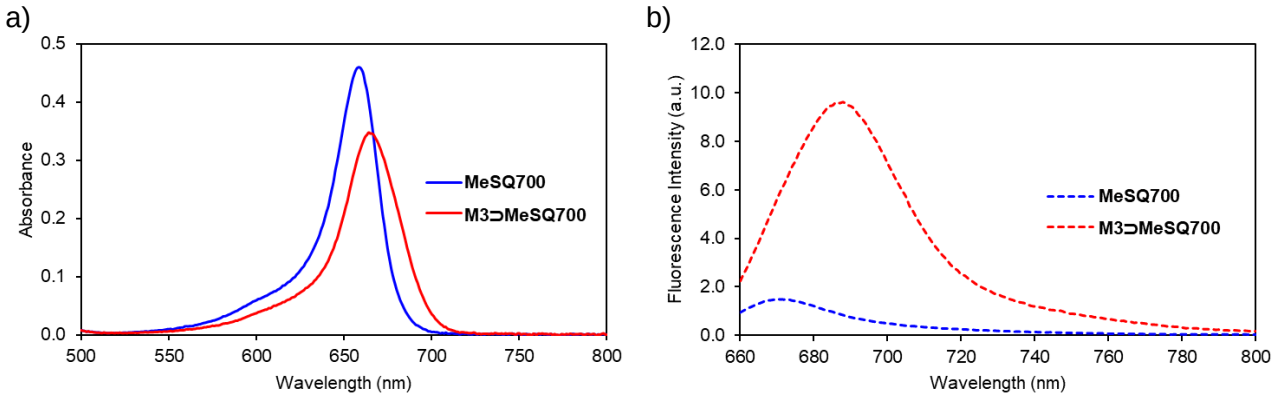

Figure S7: Changes in a) absorption and b) emission upon addition of one equivalent of **M3** to **MeSQ700** in H_2O (3.0 μM, ex. 650 nm, slit width: 2 nm at 25 °C).

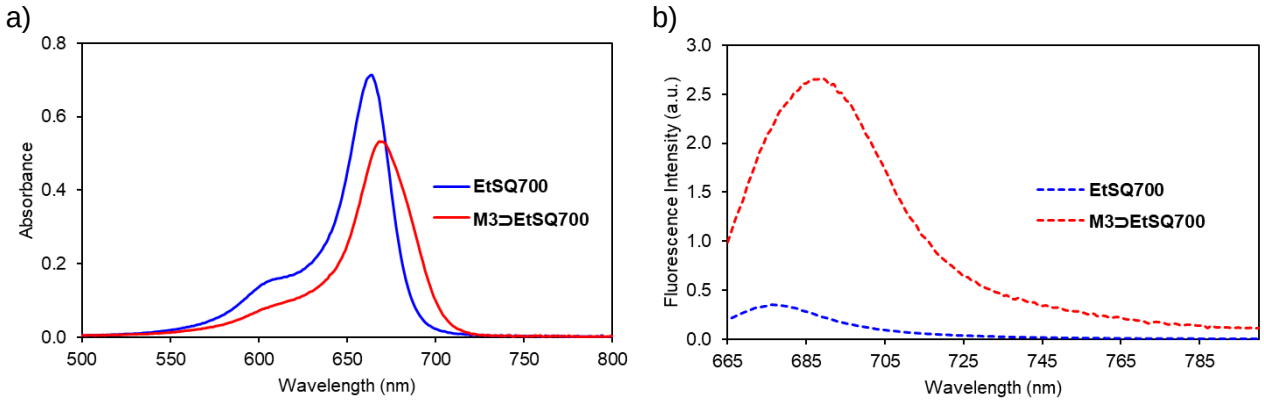

Figure S8: Changes in a) absorption and b) emission upon addition of one equivalent of **M3** to **EtSQ700** in H_2O (3.0 μM, ex. 650 nm, slit width: 2 nm at 25 °C).

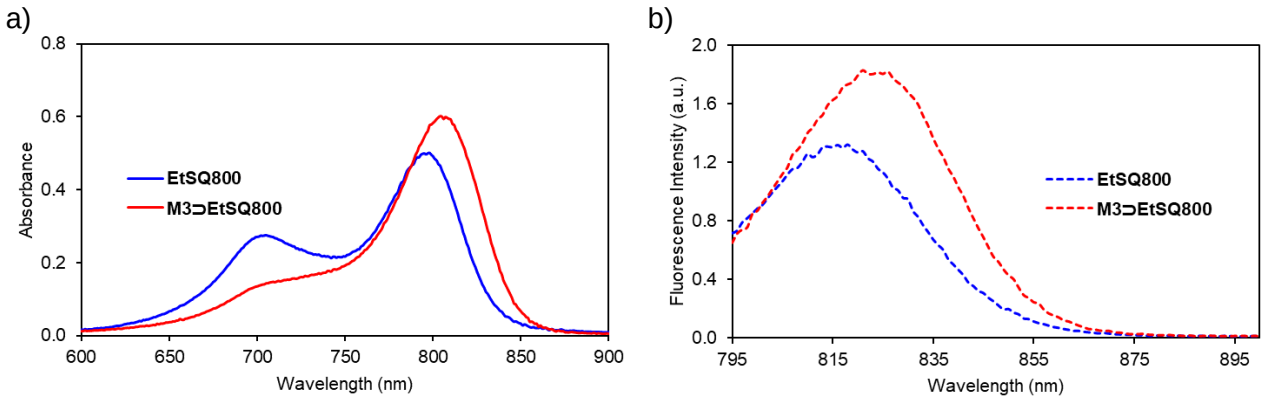

Figure S9: Changes in a) absorption and b) emission upon addition of one equivalent of **M3** to **EtSQ800** in H_2O (3.0 μM, ex. 785 nm, slit width: 3 nm at 25 °C).

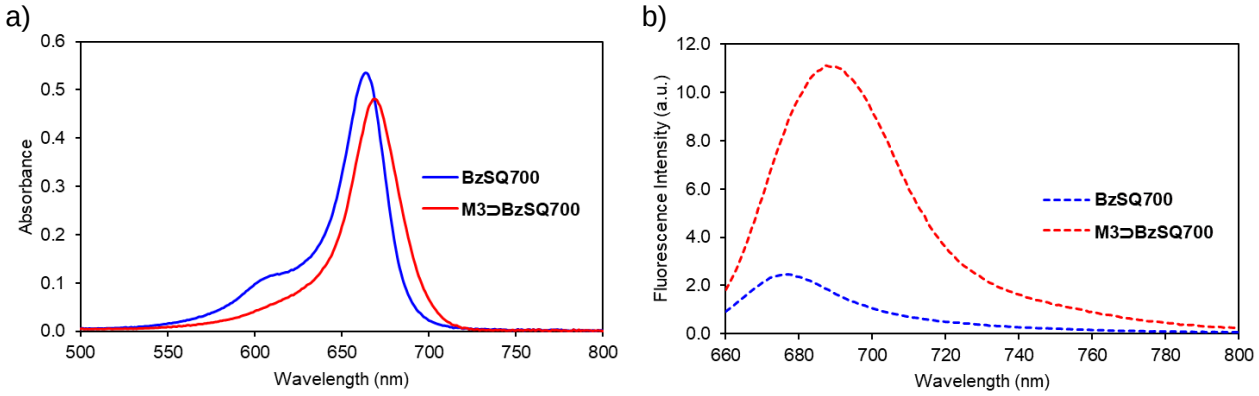

Figure S10: Changes in a) absorption and b) emission upon addition of one equivalent of **M3** to **BzSQ700** in H_2O (3.0 μM, ex. 650 nm, slit width: 2 nm at 25 °C).

Table S1: Photophysical data for squaraine dyes and complexes with **M3** in H_2O (3.0 μM) as compared to previously published complexes with **M1**.[a]

Compound	λ_{abs} (nm)	λ_{em} (nm)	log ε	Φ_f[b]
MeSQ700	658	670	5.184	0.03
M3⊃MeSQ700	664	688	5.063	0.22
M1⊃MeSQ700	675	704	-	0.14
EtSQ700	663	679	5.377	0.03
M3⊃EtSQ700	668	689	5.250	0.13
M1⊃EtSQ700	678	714	-	0.27
EtSQ800	796	819	5.173	0.07
M3⊃EtSQ800	804	829	5.242	0.10
M1⊃EtSQ800	809	829	-	0.11
BzSQ700	664	677	5.252	0.03
M3⊃BzSQ700	668	687	5.205	0.25
M1⊃BzSQ700	676	718	-	0.11

[a]Data for complexes with **M1** taken from references S5-S8.
[b]An absorbance of 0.080 and methylene blue (Φ_f = 0.02 in H_2O) or indocyanine green (Φ_f = 0.053 in H_2O) were used as standards for quantum yield measurements.

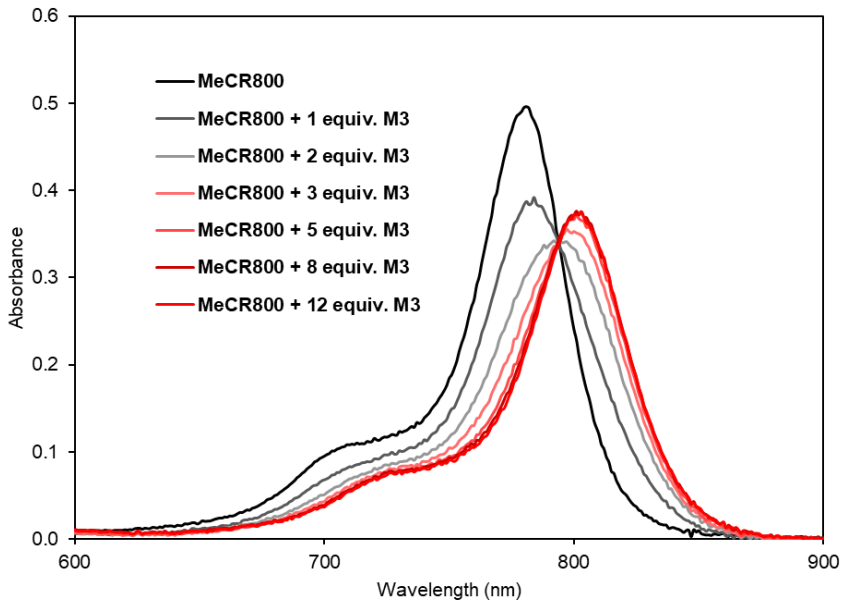

Figure S11: Titration of **MeCR800** (3.0 μM) with 0-12.0 equivalents of **M3** in H_2O.

Table S2: Photophysical data for croconaine dye with **M3** in H_2O (3.0 μM) as compared to previously published complex with **M1**.

Compound	λ_{abs} (nm)	log ε
MeCR800	781	5.218
M3⊃MeCR800	808	5.116
M1⊃MeCR800	816	-

Changes in ^{1}H NMR Spectral Patterns

In all cases, the dye's thiophene or thienothiophene protons 1 and 2 sharpen and split into two distinct peaks corresponding to *cis* and *trans* conformations of the encapsulated squaraine. That is, the relative orientation of the dye's two thiophene or thienothiophene units is *cis* or *trans*. In addition, macrocycle proton B is shifted downfield and split into two sets of signals; the major signal is a singlet indicating that most of the encapsulated squaraine adopts a *trans* conformation with regard the orientation of two thiophene units in the dye structure.

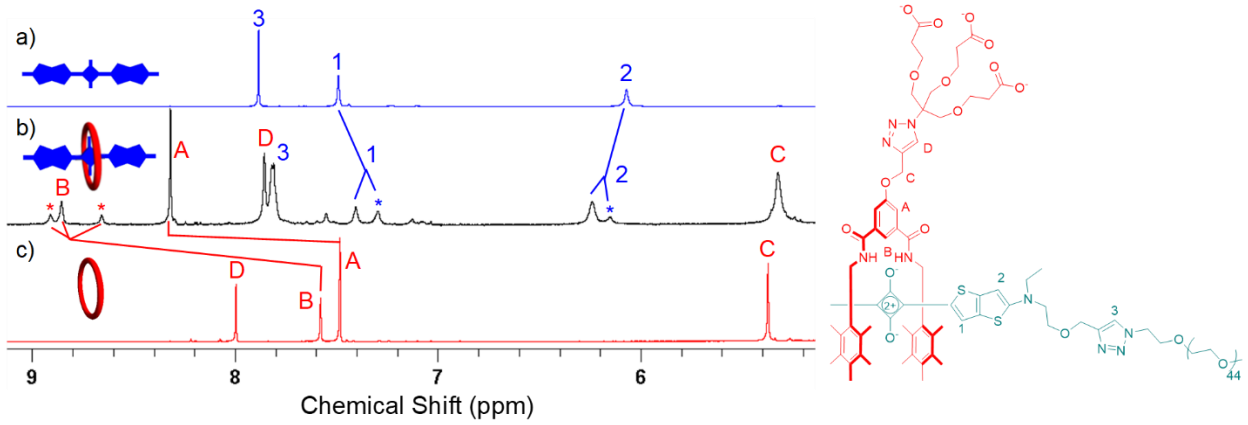

Figure S12: ^{1}H NMR (500 MHz, D_2O) of a) **EtSQ800** (1.0 mM), b) **M3⊃EtSQ800** (1.0 mM), and c) **M3** (1.0 mM). Asterisks indicate the minor complex where the thienothiophene units of **EtSQ800** are in the *cis* conformation. The small side peaks near proton 1 are residual NH signals that have not yet exchanged with the deuterated solvent.

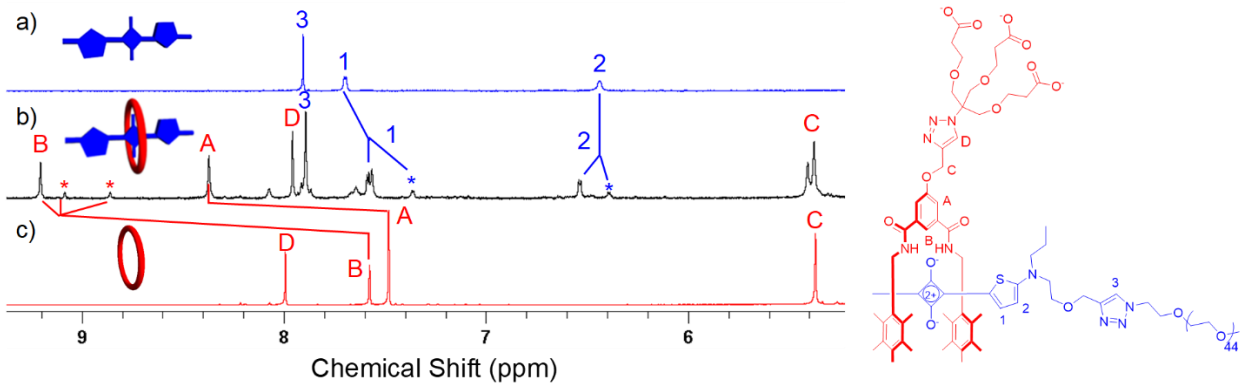

Figure S13: ^{1}H NMR (500 MHz, D_2O) of a) **PrSQ700** (1.0 mM), b) **M3⊃PrSQ700** (1.0 mM), and c) **M3** (1.0 mM). Asterisks indicate the minor complex where the thiophene units of encapsulated **PrSQ700** are in a *cis* conformation. The small unlabeled peaks near proton 1 in spectrum (b) are residual NH signals that have not yet exchanged with the deuterated solvent.

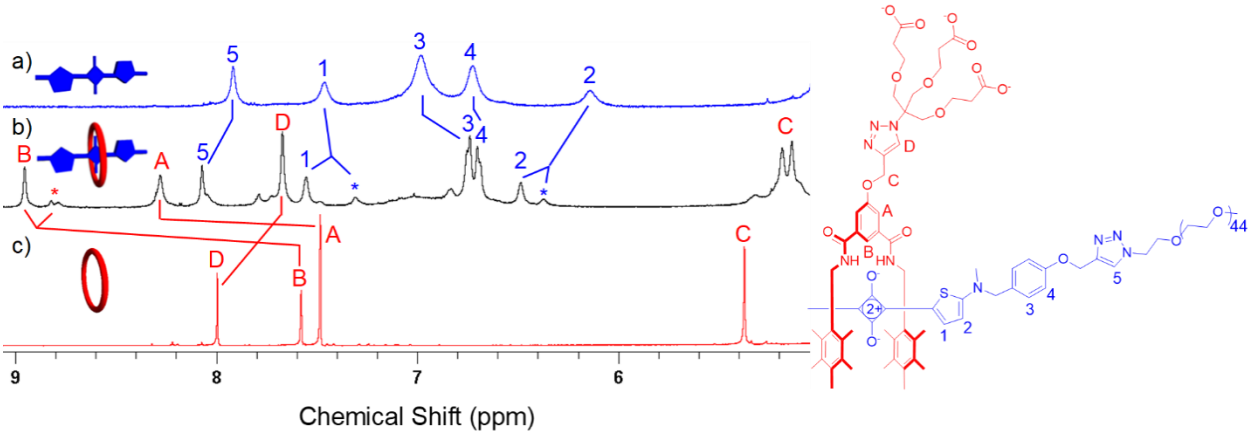

Figure S14: ^{1}H NMR (500 MHz, D_2O) of a) **BzSQ700** (1.0 mM), b) **M3⊃BzSQ700** (1.0 mM), and c) **M3** (1.0 mM). Asterisks indicate the minor complex where the thiophene units of encapsulated **BzSQ700** are in the *cis* conformation. The small unlabeled peaks in spectrum (b) are residual NH signals that have not yet exchanged with the deuterated solvent.

*2D NOESY Evidence for Guest Back-Folding in **M3⊃BzSQ700***

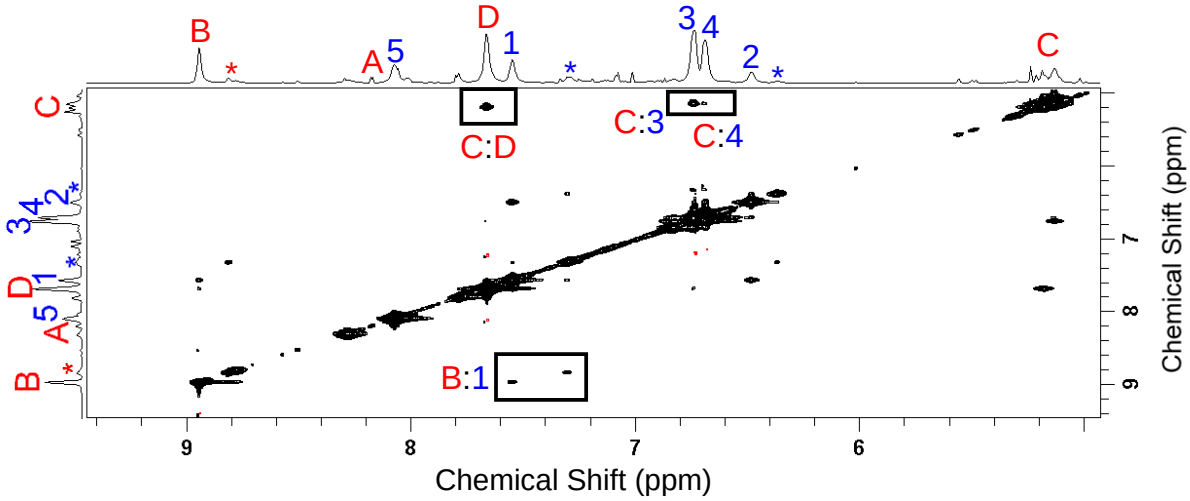

Figure S15: 2D NOESY (700 MHz, D_2O) of **M3⊃BzSQ700** (1.0 mM). Atom labels are provided in Figure S14. The interior macrocycle protons B within **M3** undergo cross-relaxation with the corresponding thiophene protons 1 of **BzSQ700** (more specifically there is a B:1 cross-relaxation peak corresponding to the dye in the major *trans* conformation and B:1 cross-relaxation peak corresponding to the dye in the minor *cis* conformation). More importantly, macrocycle methylene protons C undergo cross-relaxation with macrocycle triazole proton D (as expected) and also with benzyl protons 3 and 4 of **BzSQ700**, clear evidence for guest back-folding.

*Evidence for Formation of **M3⊃PrSQ700***

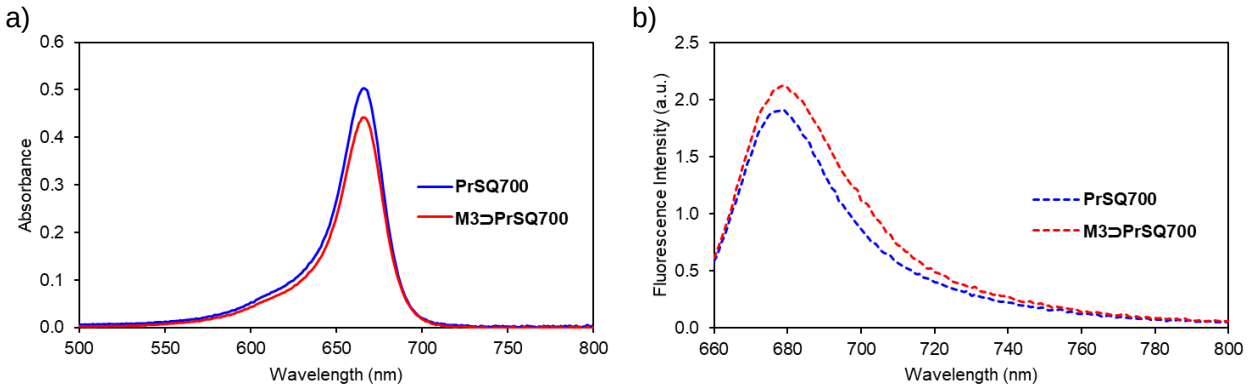

Figure S16: There is only a very small change in a) absorption and b) emission spectra for **PrSQ700** in H_2O (3.0 μM, ex. 650 nm, slit width: 2 nm at 25 °C) after addition of one equivalent of **M3** and allowing the solution to equilibrate overnight. Unambiguous evidence that **M3⊃PrSQ700** has formed was gained by the data in Figure S13 and S17.

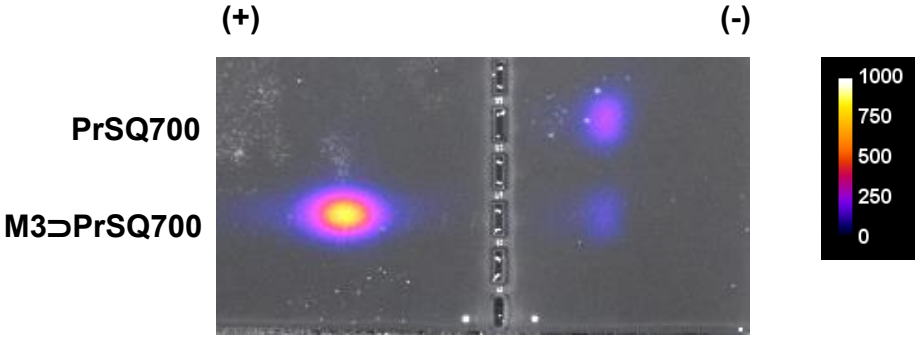

Figure S17: Agarose gel electrophoresis loaded with separate samples of **M3⊃PrSQ700** (obtained by mixing the two components) and free **PrSQ700** (100 μM/well, 2.5% agarose gel; 100 V for 30 minutes, then 110 V for 1.5 hours). Image shows the gel as photographed in ambient light, overlaid with a fluorescent image acquired with ex: 640/25 nm, em: 732/38 nm. The differences in gel migration indicate that the sample containing **M3⊃PrSQ700** has high purity and high stability.

E. Competitive Macrocycle Threading Experiments

Competitive ^{1}H NMR Macrocycle Threading Experiment

The following two sets of spectra (Figure S18) show that the B protons in **M1⊃BzSQ700** and **M3⊃BzSQ700** can easily be distinguished by chemical shift (9.5 ppm for **M1⊃BzSQ700** vs. 9.0 ppm for **M3⊃BzSQ700**). This fact enabled the competitive NMR macrocycle threading experiment in Figure S19 where a solution of **M1** was mixed with an equimolar amount of **M3⊃BzSQ700** and the ratio of **M1⊃BzSQ700** to **M3⊃BzSQ700** was measured by integration of the two diagnostic macrocycle protons B.

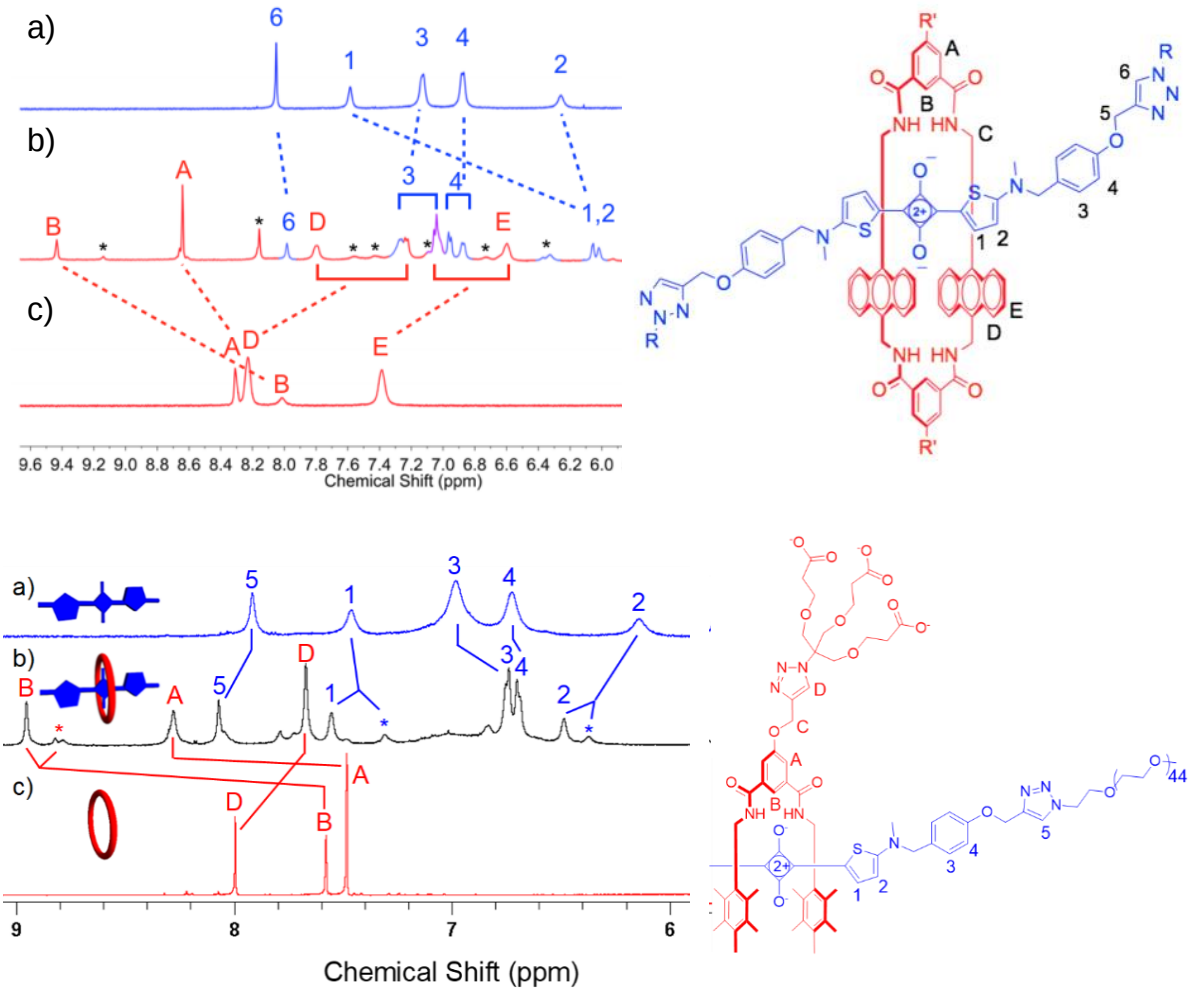

Figure S18: Partial ^{1}H NMR spectra (500 MHz, D_2O, 25 °C) of *Top:* a) **BzSQ700** (1.0 mM), b) **M1⊃BzSQ700** (1.0 mM), and c) **M1** (1.0 mM) and *Bottom:* a) **BzSQ700** (1.0 mM), b) **M3⊃BzSQ700** (1.0 mM), and c) **M3** (1.0 mM). The peaks marked * are due to the minor conformation where the dye thiophene units are in a *cis* conformation. Top figure taken from reference S8. Note that the two B protons appear at different chemical shifts (9.5 ppm for **M1⊃BzSQ700** and 9.0 ppm for **M3⊃BzSQ700**) and thus are easily distinguished in a competitive NMR experiment.

For the following competitive NMR threading experiment, the equilibrium between **M1** and **M3⊃BzSQ700** is given by

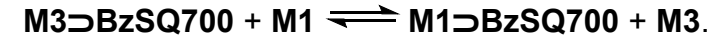

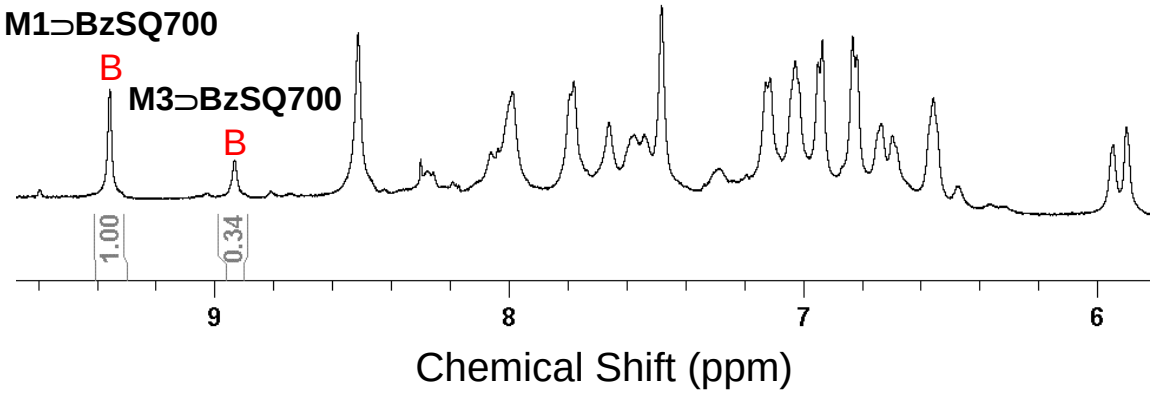

Figure S19: Partial ^{1}H NMR spectrum (500 MHz, D_2O, 25 °C) of competitive threading experiment in which **M1** is added to **M3⊃BzSQ700** (1.0 mM of each). Integration of the B proton for **M1⊃BzSQ700** and **M3⊃BzSQ700** leads to an equilibrium ratio of 1:0.34, which corresponds to a K_a value of 1 x 10^{-9} M^{-1} for formation of **M3⊃BzSQ700**, which is within error of the K_a value of (2.8 ± 2.4) x 10^{-9} M^{-1} in Table 1 obtained by fluorescence titration.

Competitive Absorption Macrocycle Threading Experiment

Absorption was used to measure the capability of **M3** to selectively bind a squaraine dye (**MeSQ700** or **BzSQ700**) in the presence of croconaine **MeCR800**.

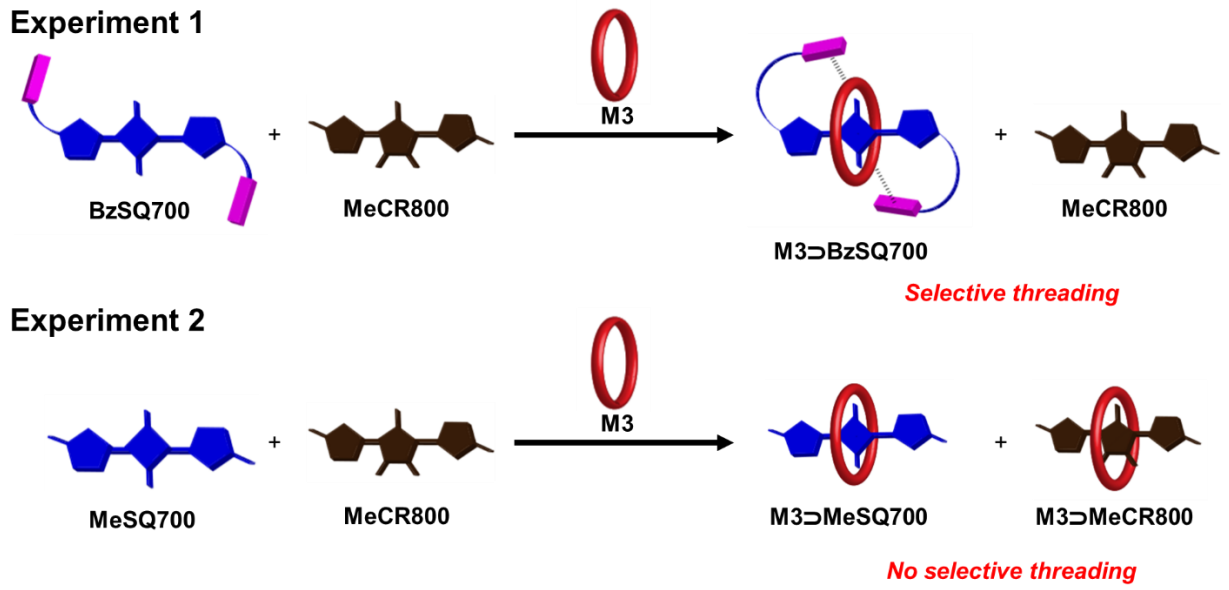

Scheme S2: Two separate absorption experiments were conducted that each added **M3** to a binary 1:1 mixture of two dyes. Experiment 1 showed that **M3** has very high selectivity for squaraine **BzSQ700** in the presence of croconaine **MeCR800** in water. In contrast, a control experiment (Experiment 2) showed that **M3** has very little selectivity for squaraine **MeSQ700** in the presence of croconaine **MeCR800**.

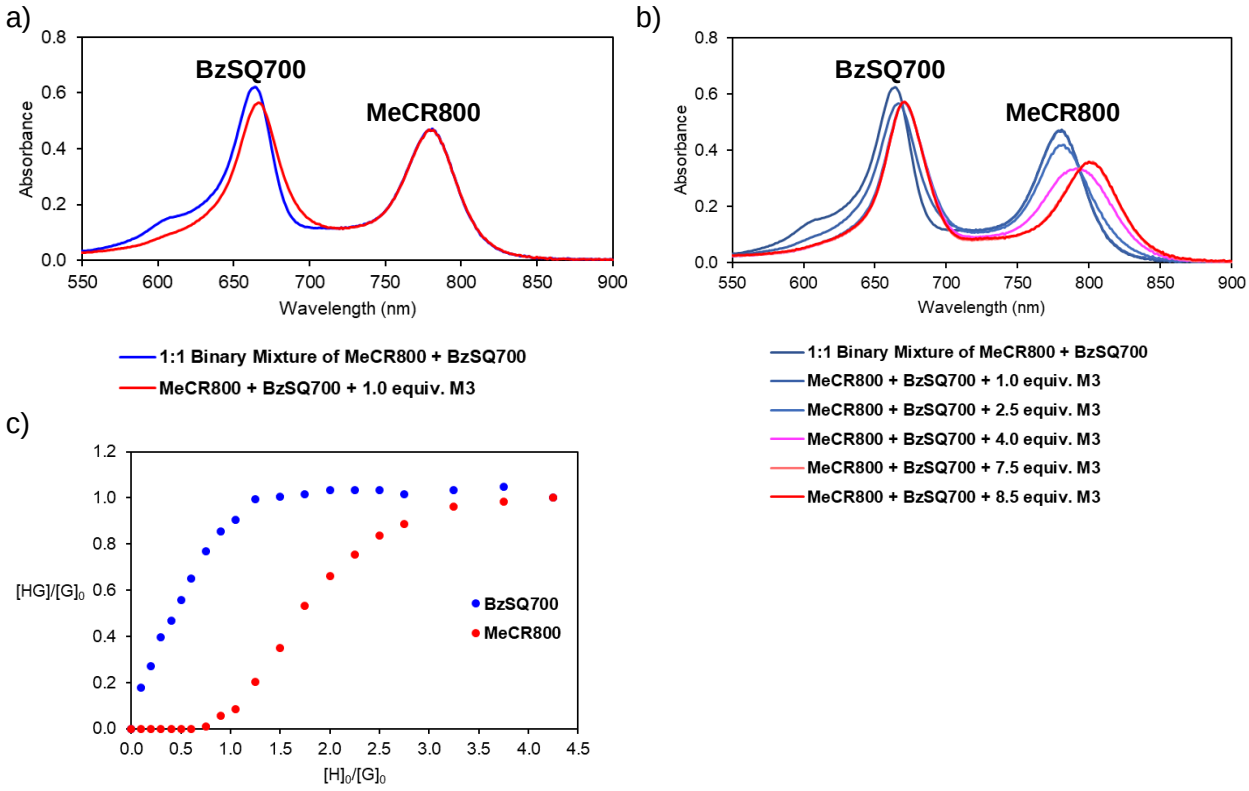

Figure S20: Data from Experiment 1 in Scheme S2. a) The first equivalent of **M3** added to a 1:1 binary mixture of **BzSQ700** and **MeCR800** (3.0 μM each) produces a red shift only in the absorption maximum of **BzSQ700**, indicative of formation of **M3⊃BzSQ700** and in good agreement with its higher affinity for **M3**. b) Following complete saturation of **BzSQ700**, the next five equivalents of **M3** were used to saturate **MeCR800** with no further red shift in the absorption maximum corresponding to **M3⊃BzSQ700**. Only six of twenty data points are shown. c) Speciation plots for competitive titration experiment that added aliquots of **M3** to a 1:1 mixture of **BzSQ700** and **MeCR800** (3.0 μM each in water) at 25 °C. The quantity along the vertical axis is the mole fraction of guest dye that is encapsulated by host **M3** and the quantity along the horizontal axis is the molar ratio of **M3** to dye.

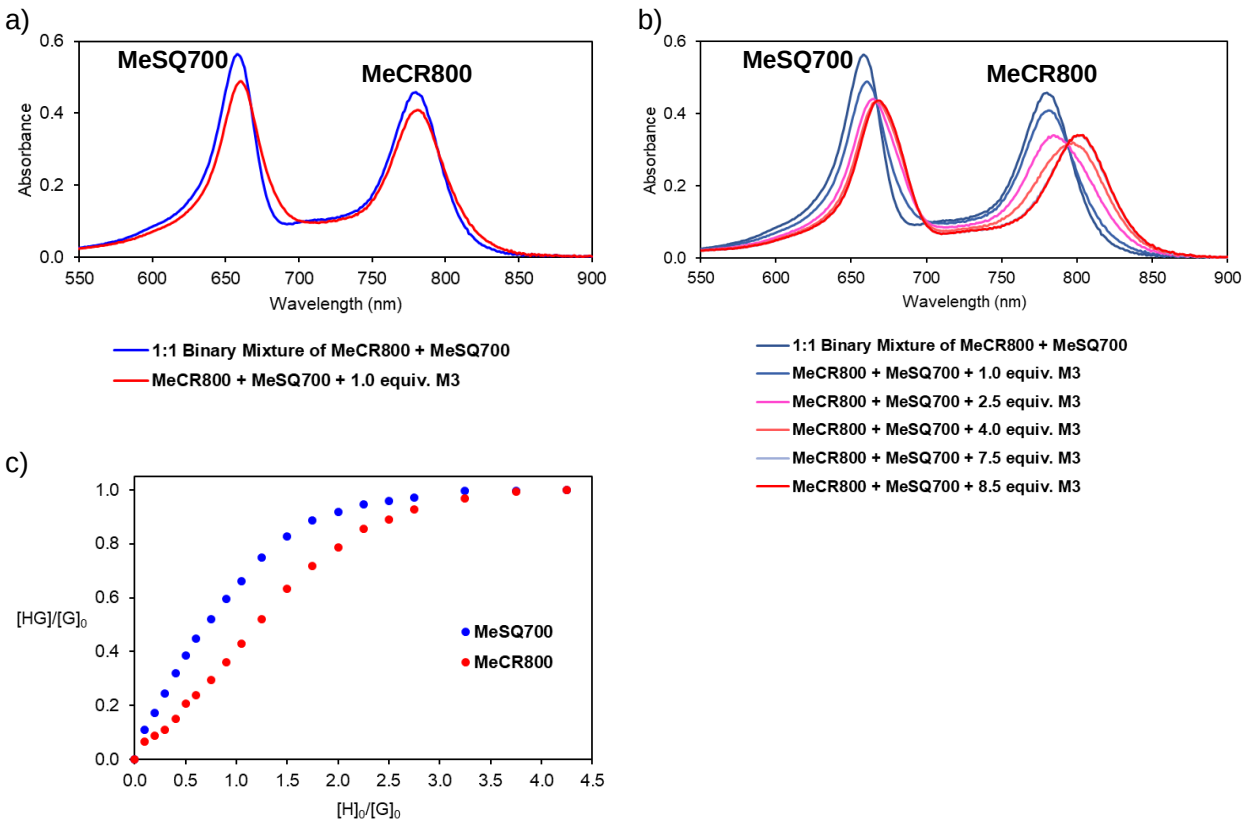

Figure S21: Data from Experiment 2 in Scheme S2. a) The first equivalent of **M3** added to a 1:1 binary mixture of **MeSQ700** and **MeCR800** (3.0 μM each) produces a red shift in the absorption maxima of both dyes, in good agreement with the dyes' similar affinities for **M3**. b) As additional equivalents of **M3** are added to a 1:1 binary mixture of **MeSQ700** and **MeCR800**, both absorption maxima continue to red-shift simultaneously. Only six of twenty data points are shown. c) Speciation plots for the control competitive titration experiment that added aliquots of **M3** to a 1:1 mixture of **MeSQ700** and **MeCR800** (3.0 μM each in water) at 25 °C. The quantity along the vertical axis is the mole fraction of guest dye that is encapsulated by host **M3** and the quantity along the horizontal axis is the molar ratio of **M3** to dye.

In Figures S20 and S21, $\frac{[HG]}{[G]_0}$ was calculated using the equation $\frac{A_t - A_0}{A_{final} - A_0}$, where A_0 is the initial absorbance of each fluorophore, A_{final} is the absorbance of the final host-guest complex, and A_t is the absorption at any time between these two points, with A_t constrained such that $A_t \geq A_0$.

F. Threading Association Constant Measurements

Algorithms for Determining K_a[S6]

For a 1:1 host-guest system:

$$H + G \underset{}{\overset{K_a}{\rightleftharpoons}} HG$$

The desired association constant is expressed in equation (1.1):

$$K_a = \frac{[HG]}{[H][G]} \quad (1.1).$$

Assigning the total concentration of host and guest as $[H]_0$ and $[G]_0$, respectively, gives mass balance equations (1.2) and (1.3).

$$[H]_0 = [H] + [HG] \quad (1.2)$$

$$[G]_0 = [G] + [HG] \quad (1.3)$$

Equation (1.2) is rearranged to define [H] and equation (1.3) is rearranged to define [G]. The newly defined [H] and [G] are used to replace [H] and [G] in equation (1.1) and the resulting equation is rearranged to yield equation (1.4):

$$[HG]^2 - ([H]_0 + [G]_0 + 1/K_a)[HG] + [H]_0[G]_0 = 0 \quad (1.4).$$

The real root of equation (1.4) is expressed in equation (1.5), which defines [HG] based on K_a and experimentally determined values ($[H]_0$ and $[G]_0$):

$$[HG] = 0.5\left\{\left([H]_0 + [G]_0 + 1/K_a\right) - \sqrt{\left([H]_0 + [G]_0 + 1/K_a\right)^2 - 4[H]_0[G]_0}\right\} \quad (1.5).$$

Fluorescence Method

A solution of 3.0 μM squaraine in H_2O was placed in a 1-mL quartz cuvette and titrated with aliquots from a macrocycle stock solution (300 μM **M3** and 3.0 μM squaraine in H_2O). Following each addition of macrocycle, a fluorescence measurement at a single point was acquired, which was then plotted to produce an isotherm that was fitted to a 1:1 binding model[S6] using Origin 8.6 software.

$[G]_t$ was kept constant and $[H]_t$ incrementally increased. The fluorescence signal was related to the concentration of [G] and [HG], assuming the host has negligible fluorescence at the wavelength studied. The fluorescence intensity can be described by equation (2.1):

$$F = k_1[G] + k_2[HG] \quad (2.1).$$

Combining equations (1.3) and (2.1) gives equation (2.2):

$$F = (k_2 - k_1)[HG] + k_1[G]_0 \quad (2.2).$$

When $[H]_t$=0,

$F_0 = k_1[G]_0$ (2.3) and

$F/F_0 = 1 + \frac{(k_2 - k_1)[HG]}{k_1[G]_0} = 1 + \frac{k[HG]}{[G]_0}$ (2.4), where k=(k_2-k_1)/k_1.

In our analysis, we treated either G_0 or H_0 as slightly adjustable to reach the best fitting, since real molar concentration is inherently dependent on a variety of experimental conditions (i.e., polydispersity of each PEG-modified dye, balance error, presence of water as an impurity both in the macrocycle and/or PEG modified-dye, photobleaching of squaraine dye). Varying this parameter, and related values in later analyses, greatly improves the accuracy of the fitting result. We define the host-guest ratio as

$\frac{[H]_0}{[G]_0} = r$ (2.5).

We further introduce the concentration correction coefficient *m* into equation (2.5):

$\frac{[H]_0}{m[G]_0} = r$ (2.6).

Combining equations (2.4), (2.6), and (1.5), we relate the fluorescence signal to concentration by

$F/F_0 = f([G]_0, r, m, k, K_a)$ (2.7),

which was used in Origin 8.6 for nonlinear fitting to obtain the association constant K_a. To better initialize the parameters, we bounded the fitted parameter within reasonable scope ($0.5<m<1.5$, $0<K_a<1000/[G]_0$). The resulting *m* value was used to correct the real concentration ratio.

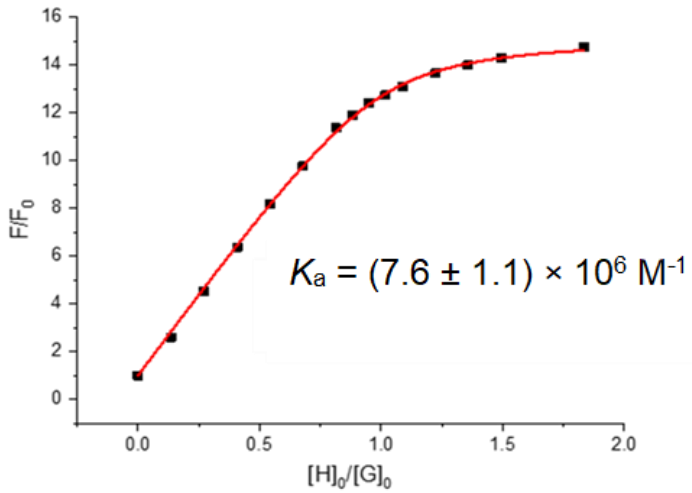

Independent Variable	Regular Residual of F/F_0
0	0
0.13579	-0.23726
0.27157	-0.13532
0.40736	-0.08829
0.54314	0.04327
0.67893	-0.00405
0.81472	0.16308
0.88261	0.09777
0.9505	0.06382
1.01839	-0.07225
1.08629	-0.08974
1.22207	-0.07798
1.35786	-0.07869
1.49365	-0.01529
1.83311	0.13712

Figure S22: Representative titration of 3.0 μM **MeSQ700** with increasing equivalents of **M3** in H_2O fitted to a 1:1 binding model (ex. 650 nm, em. 690 nm, slit width: 2 nm at 25 °C). K_a is the average and standard deviation of three independent measurements.

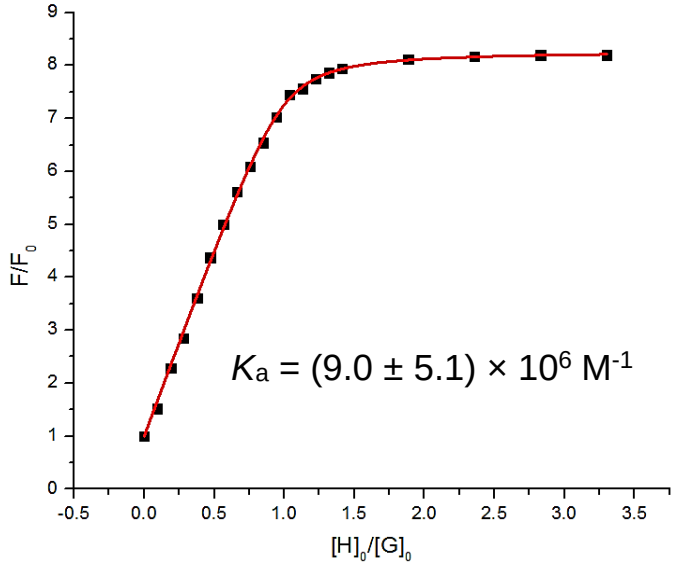

Independent Variable	Regular Residual of F/F_0
0	0
0.09429	-0.14929
0.18858	-0.0471
0.28287	-0.14304
0.37716	-0.04599
0.47145	0.0796
0.56574	0.07432
0.66003	0.08057
0.75432	-0.00607
0.84861	-0.07302
0.9429	-0.01922
1.03719	0.07283
1.13148	-0.04066
1.22577	-0.01457
1.32006	4.69763E-4
1.41435	0.00114
1.8858	0.01401
2.35725	0.00331
2.8287	0.0084
3.30015	-0.01158

Figure S23: Representative titration of 3.0 μM **EtSQ700** with increasing equivalents of **M3** in H_2O fitted to a 1:1 binding model (ex. 650 nm, em. 690 nm, slit width: 2 nm at 25 °C). K_a is the average and standard deviation of three independent measurements.

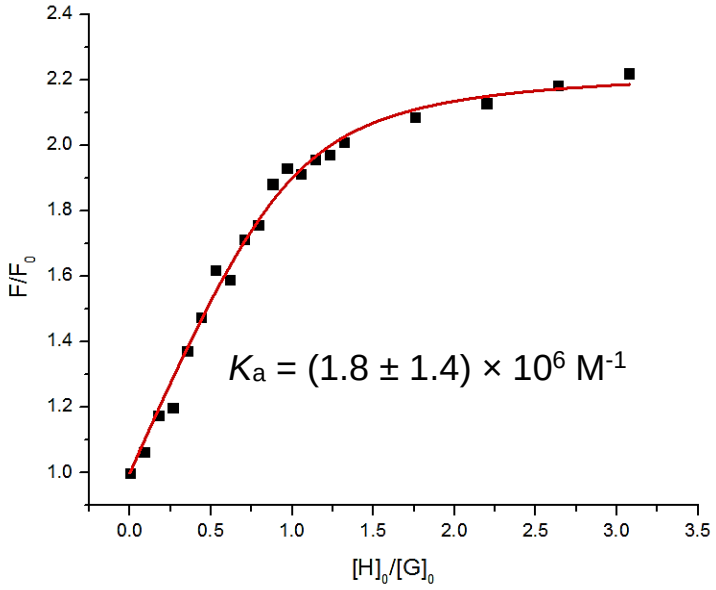

Independent Variable	Regular Residual of F/F_0
0	0
0.08788	-0.03435
0.17577	-0.01979
0.26365	-0.08978
0.35154	-0.00833
0.43942	0.00797
0.5273	0.0675
0.61519	-0.03985
0.70307	0.00864
0.79096	-0.01405
0.87884	0.05181
0.96672	0.04841
1.05461	-0.01467
1.14249	-0.00829
1.23038	-0.02579
1.31826	-0.01482
1.75768	-0.02447
2.1971	-0.02044
2.63652	0.01118
3.07594	0.03335

Figure S24: Representative titration of 3.0 μM **EtSQ800** with increasing equivalents of **M3** in H_2O fitted to a 1:1 binding model (ex. 806 nm, em. 830 nm, slit width: 3 nm at 25 °C). K_a is the average and standard deviation of three independent measurements.

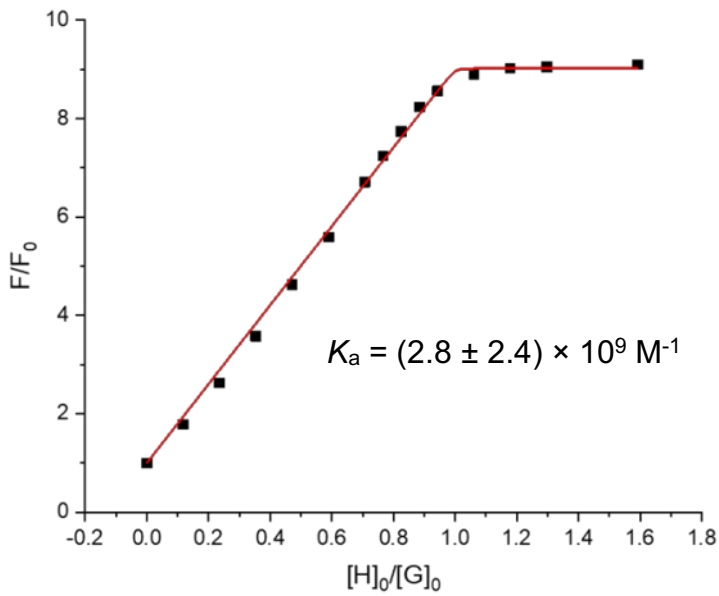

Independent Variable	Regular Residual of F/F_0
0	0
0.1179	-0.16133
0.2358	-0.26181
0.35369	-0.26195
0.47159	-0.15289
0.58949	-0.13818
0.70739	0.03935
0.76634	0.09485
0.82529	0.11922
0.88423	0.14178
0.94318	0.00546
1.06108	-0.11341
1.17898	0.0033
1.29688	0.03043
1.59162	0.07721

Figure S25: Representative titration of 3.0 μM **BzSQ700** with increasing equivalents of **M3** in H_2O fitted to a 1:1 binding model (ex. 650 nm, em. 690 nm, slit width: 2 nm at 25 °C). K_a is the average and standard deviation of four independent measurements.

Absorption Method

A solution of 3.0 μM croconaine in H_2O was placed in a 1-mL quartz cuvette and titrated with aliquots from a macrocycle stock solution (300 μM **M3** and 3.0 μM croconaine in H_2O). Following each addition of macrocycle, an absorption spectrum was acquired. Both the decrease in absorption of the free croconaine and the increase in absorption due to formation of the complex were then plotted to produce isotherms that were fitted to a 1:1 binding model[S6] using Origin 8.6 software.

According to Beer's law,

$$A = \varepsilon_H b[H] + \varepsilon_G b[G] + \varepsilon_{HG} b[HG] \quad (3.1).$$

If at the selected wavelength, ε_H=0, then equation (3.1) can be simplified as equation (3.2):

$$A = \varepsilon_G b[G] + \varepsilon_{HG} b[HG] \quad (3.2).$$

According to equation (1.3), [G] can be defined by $[G]_0$ and [HG], thus (3.2) gives equation (3.3):

$$A = \varepsilon_G b[G]_0 + (\varepsilon_{HG} - \varepsilon_G) b[HG] \quad (3.3).$$

At the beginning of the titration,

$A_0 = \varepsilon_G b[G]_0$ (3.4), then

$\Delta A = A - A_0 = (\varepsilon_{HG} - \varepsilon_G) b[HG] = \varepsilon b[HG]$ (3.5), where $\varepsilon = \varepsilon_{HG} - \varepsilon_G$.

From Equation (1.5) and (3.5), we get

$\Delta A = f([H]_0, [G]_0, \varepsilon, K_a)$ (3.6).

Here we established the relationship between absorption data ΔA, the concentrations $[H]_0$ and $[G]_0$, the absorption coefficients ε_{HG} and ε_G, and the association constant K_a. From equations (3.6) and (2.6), we get

$\Delta A = f([G]_0, r, m, \varepsilon, K_a)$ (3.7),

which was used for the nonlinear fitting in Origin 8.6 to obtain the association constant K_a.

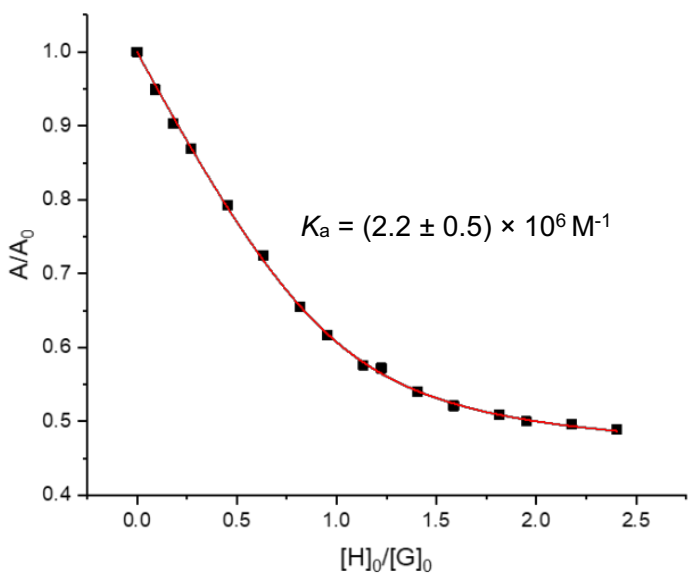

Independent Variable	Regular Residual of A/A_0
0	1
0.09067	0.3638
0.18134	0.31719
0.272	0.28329
0.45334	0.20702
0.63468	0.13923
0.81601	0.06931
0.95201	0.03118
1.13335	-0.00908
1.22402	-0.01332
1.40535	-0.0451
1.58669	-0.06416
1.81336	-0.07688
1.94936	-0.08535
2.17603	-0.08959
2.4027	-0.09594

Figure S26: Representative titration of 3.0 μM **MeCR800** with increasing equivalents of **M3** in H_2O with the decrease in free croconaine absorption fitted to a 1:1 binding model. K_a is the average and standard deviation of three independent measurements.

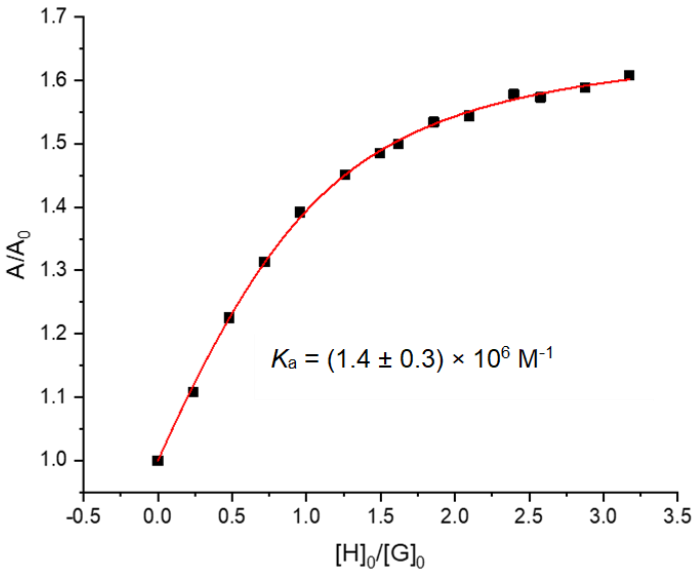

Independent Variable	Regular Residual of A/A_0
0	0
0.09327	-0.00133
0.18655	-0.01442
0.27982	8.07361E-4
0.46637	-0.00218
0.65292	0.00964
0.83947	-0.00181
0.97938	0.00233
1.16593	0.00349
1.2592	-0.00528
1.44575	0.00576
1.6323	-0.01178
1.86548	0.0119
2.00539	-0.01547
2.23858	-0.00184
2.47176	0.01029

Figure S27: Representative titration of 3.0 μM **MeCR800** with increasing equivalents of **M3** in H_2O with the increase in croconaine-macrocycle complex absorption fitted to a 1:1 binding model. K_a is the average and standard deviation of three independent measurements.

Table S3: Association constants for croconaine dye threading of **M3** in H_2O (3.0 μM) and threading of **M1**.[a]

Complex formed	K_a (M^{-1})	Method
M3⊃MeCR800	$(2.2 \pm 0.5) \times 10^6$	Fitting decrease in free croconaine absorbance
M3⊃MeCR800	$(1.4 \pm 0.3) \times 10^6$	Fitting increase in macrocycle-croconaine complex
M1⊃MeCR800	$(1.4 \pm 0.2) \times 10^9$	

[a] Association constant for threading of **M1** taken from reference S9.

G. Threading Rate Constant Measurements

Algorithms for the determination of k_{on}[S6]

For a second order reaction,

$$H + G \underset{k_{off}}{\overset{k_{on}}{\rightleftharpoons}} HG$$

The reaction rate can be written as

$$Rate = -\frac{d[G]}{[G]} = k_{on}[H][G] - k_{off}[HG] = k_{on}[H][G] - \frac{k_{on}}{K_a}[HG] \quad (4.1).$$

For a strong association system where K_a >100 M^{-1}, the contribution of the reverse reaction on the reaction rate is negligible, so equation (4.1) can be simplified as (4.2):

$$Rate = -\frac{d[G]}{[G]} = k_{on}[H][G] \quad (4.2).$$

In the case where $[H]_0$=$[G]_0$, since H and G react with a 1:1 stoichiometry, [H] = $[H]_0$ - x and [G] = $[G]_0$ - x. At any time t, [H]=[G] and equation (4.2) can be further simplified as (4.3):

$$Rate = -\frac{d[G]}{[G]} = k_{on}[G]^2 \quad (4.3).$$

Solving the differential rate equation (4.3) gives the integrated rate equation (4.4):

$$\frac{1}{[G]_t} - \frac{1}{[G]_0} = k_{on}t \quad (4.2).$$

Fluorescence Method

An aliquot of macrocycle solution (1.0-4.0 molar equivalents) in H_2O was added to a solution of 3.0 μM squaraine in H_2O and the increase in fluorescence intensity at a single wavelength (due to formation of the threaded complex) was monitored over time. Kinetic studies for N-methyl and N-benzyl squaraines were performed by using an SFA-20M stopped-flow device (empirical dead time < 8 ms). Equal volumes of host solution and guest solution were mixed by the stopped-flow device. The kinetic curves were then fitted to second-order kinetic model[S6] using Origin 8.6 software.

Either equimolar solutions of the host and guest were mixed or excess host was added as noted, and the fluorescence signal was related to the concentration of [G] and [HG], assuming the host has negligible fluorescence at the wavelength studied. The fluorescence intensity can be described by equation (5.1):

$$F = k_1[G] + k_2[HG] \quad (5.1).$$

When t=0,

$$F_0 = k_1[G]_0 \quad (5.2).$$

Combining equations (1.3), (5.1) and (5.2) gives equation (5.3):

$$F/F_0 = 1 + \frac{(k_2 - k_1)[HG]}{k_1[G]_0} \quad (5.3).$$

Combining equation (1.3) and equation (4.4) gives equation (5.4) :

$$\frac{1}{[G]_0 - [HG]} - \frac{1}{[G]_0} = k_{on} t \quad (5.4).$$

Replacing [HG] in equation (5.4) with equation (5.3) gives equation (5.5), which describes the relationship between fluorescence and time:

$$F/F_0 = 1 + \frac{k_2 - k_1}{k_1}\left(1 - \frac{1}{k_{on} t[G]_0 + 1}\right) \quad (5.5).$$

Equation (5.5) was used in Origin 8.6 for nonlinear fitting. The association rate k_{on} can be determined by using the increase in fluorescence intensity over time and nonlinear regression analysis.

In the case where the guest molecule is also transparent, the fluorescence intensity can be described by equation (5.6):

$$F = k_2[HG] \quad (5.6).$$

Replacing [HG] in equation (5.4) with equation (5.6) gives equation (5.7):

$$F = k_2 G_0\left(1 - \frac{1}{k_{on} t[G]_0 + 1}\right) \quad (5.7).$$

Equation (5.7) is used in Origin 8.6 for nonlinear fitting to determine the rate constant k_{on}.

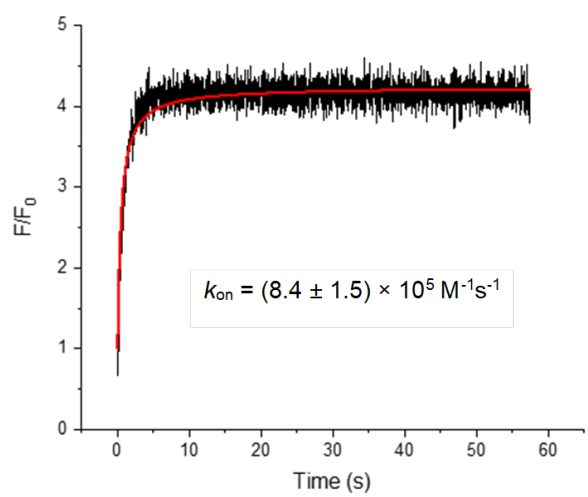

Figure S28: Representative curve for association of 3.0 μM **MeSQ700** with 1.0 equivalent **M3** in H_2O fitted to second-order kinetics (ex. 650 nm, em. 690 nm, slit width: 2 nm at 25 °C). k_{on} is the average and standard deviation of three independent measurements.

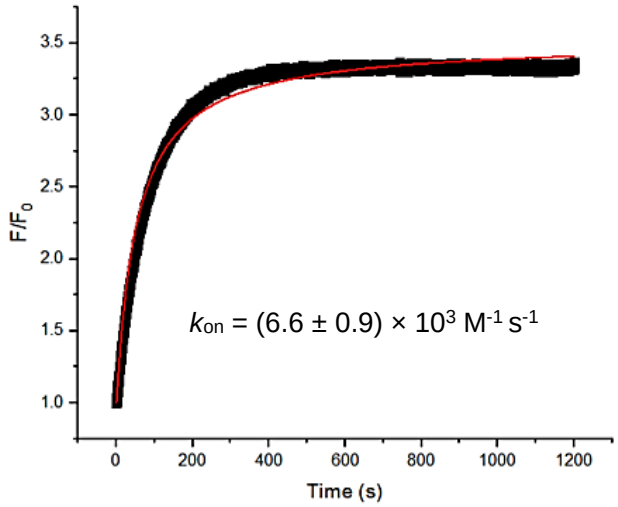

Figure S29: Representative curve for association of 3.0 μM **EtSQ700** with 3.5 equivalents **M3** in H_2O fitted to second-order kinetics (ex. 650 nm, em. 690 nm, slit width: 2 nm at 25 °C). k_{on} is the average and standard deviation of three independent measurements.

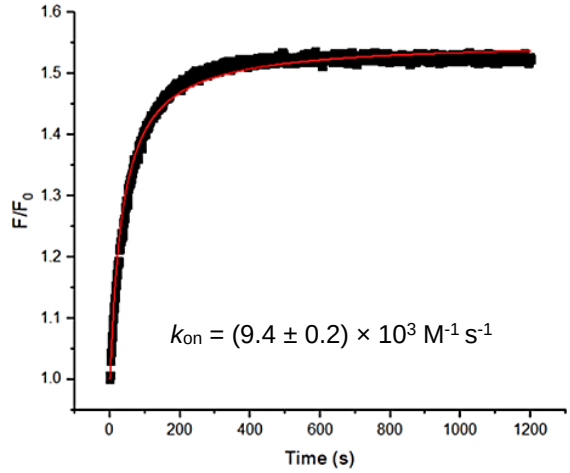

Figure S30: Representative curve for association of 3.0 μM **EtSQ800** with 3.5 equivalents **M3** in H_2O fitted to second-order kinetics (ex. 806 nm, em. 830 nm, slit width: 3 nm at 25 °C). k_{on} is the average and standard deviation of three independent measurements.

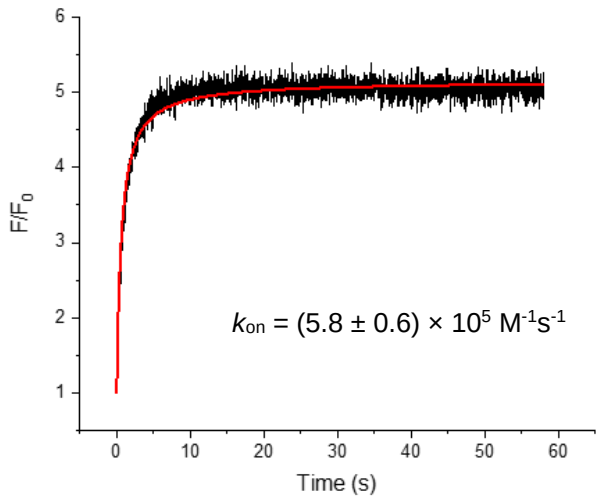

Figure S31: Representative curve for association of 3.0 μM **BzSQ700** with 1.0 equivalent **M3** in H_2O fitted to second-order kinetics (ex. 650 nm, em. 690 nm, slit width: 2 nm at 25 °C). k_{on} is the average and standard deviation of three independent measurements.

H. Molecular Dynamics Simulations of Threaded Complex

The ESI contains a movie file <**MDcomplex_M3_BzSQ700.avi**> that shows 1000 snapshots from a 100 ns Molecular Dynamics (MD) simulation of a complex comprised of host **M3** threaded by a truncated version of **BzSQ700**. The simulation procedure has been described before.[S8] In short, the MD simulations were started from DFT optimized structures and the *xleap* module was used to set up each calculation. A TIP3P water box extending 12 Å in each direction was added and NAMD (version 2.11) was used to perform the MD simulations with the gaff2 force field. A cut-off of 10 Å was used for the treatment of non-bonded interactions. Prior to the MD simulations, a two-step minimization procedure was used. First, the solvent was minimized while constraining the solute. Then, the entire system was minimized over 5000 conjugate gradient steps. Heating to 300 K was performed in the NVT ensemble with constraints on the solute. This was followed by 100 ns NPT production runs. Simulations used 2 fs time steps and the SHAKE algorithm was used to constrain bonds between heavy atoms and hydrogen. Coordinates were written every picosecond.

I. References

S1. W. Liu, A. G. Oliver and B.D. Smith, *J. Am. Chem. Soc.*, 2018, **140**, 6810–6813.

S2. S. K. Shaw, W. Liu, C. F. A. Gómez-Durán, C. L. Schreiber, M. de L. Betancourt Mendiola, C. Zhai, F. M. Roland, S. J. Padanilam and B. D. Smith, *Chem. - A Eur. J.*, 2018, **24**, 13821–13829.

S3. C. F. A. Gómez-Durán, W. Liu, M. de L. Betancourt-Mendiola and B. D. Smith, *J. Org. Chem.*, 2017, **82**, 8334–8341.

S4. C. Ke, H. Destecroix, M. P. Crump and A. P. Davis, *Nat. Chem.*, 2012, **4**, 718–723.

S5. W. Liu, E. M. Peck, K. D. Hendzel and B. D. Smith, *Org. Lett.*, 2015, **17**, 5268–5271.

S6. E. M. Peck, W. Liu, G. T. Spence, S. K. Shaw, A. P. Davis, H. Destecroix and B. D. Smith, *J. Am. Chem. Soc.*, 2015, **137**, 8668–8671.

S7. W. Liu, H. H. McGarraugh and B. D. Smith, *Molecules*, 2018, **23**, 2229.

S8. W. Liu, A. Johnson and B. D. Smith, *J. Am. Chem. Soc.*, 2018, **140**, 3361–3370.

S9. W. Liu, E. M. Peck and B. D. Smith, *J. Phys. Chem. B*, 2016, **120**, 995–1001.